# Buckling tests on plate girders

Autor(en): **Basler, Konrad / Thürlimann, Bruno**

Objekttyp: **Article**

Zeitschrift: **IABSE congress report = Rapport du congrès AIPC = IVBH Kongressbericht**

Band (Jahr): **6 (1960)**

PDF erstellt am: **13.07.2024**

Persistenter Link: https://doi.org/10.5169/seals-7011

## VI 7

# Buckling Tests on Plate Girders

*Essais de voilement sur poutres à âme pleine*

*Beulversuche an Vollwandträgern*

KONRAD BASLER BRUNO THÜRLIMANN
Fritz Engineering Laboratory, Lehigh University, Bethlehem, Pennsylvania, U.S.A.

## 1. Introduction

At present the design of plate girder webs is based on the classical buckling theory. According to this theory sudden lateral deflection of the web should occur when the buckling load is reached. It is well known that, for a column, this load practically coincides with its ultimate load. Plates, however, exhibit a post-buckling strength. This holds especially to the webs of plate girders as recent tests have shown, Ref. [1] to [5]. Specifications recognize the inherent post-buckling strength by assigning relatively low factors of safety. This practice is rather disquieting for these safety factors are determined arbitrarily without due recourse to the actual load carrying capacity of plate girders. It has been pointed out repeatedly that there exists a lack of information concerning their strength, e. g. Ref. [6]. It becomes apparent that answers to the following two problems are required:

What is the carrying capacity of plate girders?
Does the classical buckling theory furnish any significant predictions concerning the actual behavior of plate girder webs?

In order to study the strength of plate girders beyond the computed web buckling load, a number of full-size girders were tested at Fritz Engineering Laboratory. It is expected that the results, together with a theoretical study, will lead to general predictions of the static load carrying capacity of thin-web plate girders. A comprehensive report on the experimental investigation is being prepared.

The scope of this report is to present the most significant test results. These results will show that the classical buckling theory is unable to predict the behavior of plate girders fabricated according to standard shop practices. Furthermore, they will show that this theory can not be used as a basis for ultimate load predictions.

## 2. Design of Test Girders

A careful review of the pertinent literature and an analysis of the different problems involved preceded the design of the girders, Ref. [10]. For proper appreciation of the test results it is helpful to state the considerations which led to the design of the girders and describe the manner in which they were tested.

Of all possible parameters influencing the carrying capacity of plate girders, the investigation was restricted to the following four: (1) shape of the compression flange, (2) slenderness of the web, (3) ratio of shear to bending stress, and (4) spacing of the transverse stiffeners. Since a girder necessarily contains all four parameters, it was obvious that a single test on a single girder would not show experimentally the relative influence of these parameters. This necessitated conducting a number of tests where only one parameter was varied in order to obtain clear evidence of its influence. Testing conditions were chosen such that all undesired influences could be eliminated. Thus, the possibility of lateral torsional buckling of the girder was avoided by adequate lateral bracing. The loading and reaction points were clearly separated from the test section. Finally, the dimensions of the girders were chosen such that conventional material sizes and standard fabrication methods could be used.

These considerations resulted in the design of seven test girders illustrated in fig. 1. The parametric values, the actual dimensions, and the yield stress of the material are listed in table 1. Each girder consisted of a test section and two end sections with a heavier web. Thus failure was forced to occur somewhere in the test sections, which were subjected to clearly defined loadings. The test sections of girders No. 1 to 5, referred to as bending girders (fig. 1a), were subjected to pure bending. On the other hand, the center of the test sections of girders No. 6 and 7, referred to as shear girders (fig. 1b), was under pure shear. In this way the two most extreme loading conditions were produced.

Fig. 1c shows the three cross sections selected to get an appropriate variation of the first parameter, the shape of the compression flange. This figure, together with the information in table 1, allows a comparison between the bending girders. Girder No. 2, a conventionally designed plate girder, is flanked on one side by girder No. 1 with a plate-like top flange, and on the other side by girder No. 3 with a tubular top flange. Girders No. 4 and 5 are identical with girders No. 2 and 3 except for an increase in the web slenderness ratio from $b/t = 185$ to $b/t = 388$.

By subdividing the test section into two short and one long panel, a varia-

Fig. 1a

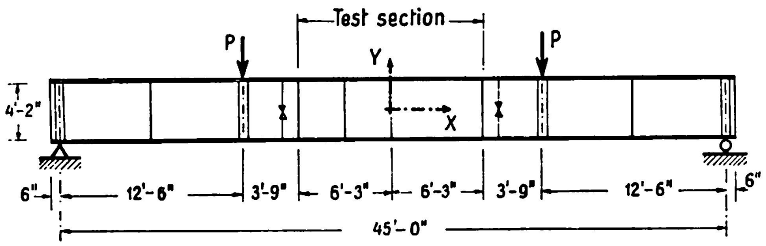


Fig. 1b

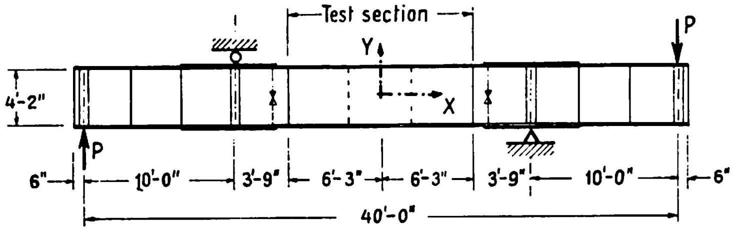


Fig. 1c

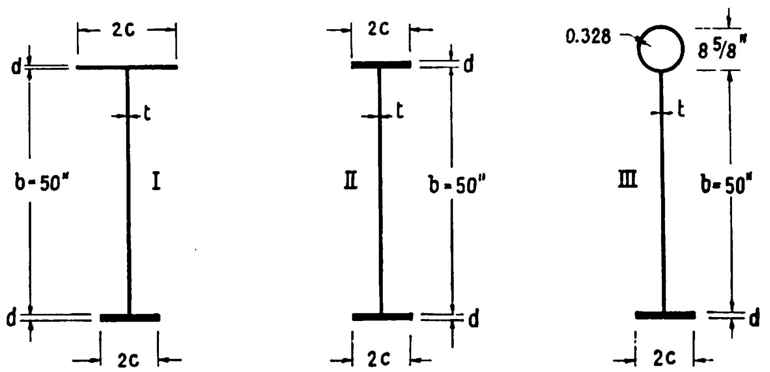


Fig. 1. Bending Girders No. 1 to 5 (Fig. 1a). Shear Girders No. 6 and 7 (Fig. 1b). Cross Sections I, II, III (Fig. 1c).

*Table 1. Summary of Girder Properties*

| Girder No. | | | 1 | 2 | 3 | 4 | 5 | 6 | 7 |
|---|---|---|---|---|---|---|---|---|---|
| | | | | | | Parameters | | | |
| Type of cross section (Fig. 1c) | | | I | II | III | II | III | II | II |
| Web slenderness | | $\beta = b/t$ | 185 | 185 | 185 | 388 | 388 | 259 | 255 |
| Loading condition | | $\zeta = \tau/\sigma$ | 0 | 0 | 0 | 0 | 0 | $\infty$ | $\infty$ |
| Panel ratio | | $\alpha = a/b$ | 1.50 | 1.50 | 1.50 | 1.50 | 1.50 | 1.50 | 1.00 |
| | | | 0.75 | 0.75 | 0.75 | 0.75 | 0.75 | 0.75 | |
| | | | | | | | | 0.50 | |
| | | | | | | Dimensions in inches | | | |
| Top flange | width | 2c | 20.56 | 12.19 | 8.625 | 12.16 | 8.625 | 12.13 | 12.19 |
| | thickness | d | 0.427 | 0.769 | 0.328 | 0.774 | 0.328 | 0.778 | 0.769 |
| Bottom flange | width | 2c | 12.25 | 12.19 | 12.19 | 12.19 | 12.25 | 12.13 | 12.19 |
| | thickness | d | 0.760 | 0.774 | 0.770 | 0.765 | 0.767 | 0.778 | 0.766 |
| Web thickness | test sect. | t | 0.270 | 0.270 | 0.270 | 0.129 | 0.129 | 0.193 | 0.196 |
| | end sect. | t | 0.382 | 0.507 | 0.492 | 0.392 | 0.392 | 0.369 | 0.381 |
| Cover plates | width | | | | | | | 11.19 | 11.19 |
| | thickness | | | | | | | 0.510 | 0.510 |
| Yield stress in ksi | | | 35.4 | 38.6 | 35.5 | 37.6 | 35.5 | 36.7 | 36.7 |

tion in stiffener spacing was obtained for the bending girders. It was anticipated that a first test would produce failure in the long panel. Upon reinforcing, a second test would lead to failure in one of the short panels. For shear loading two equal girders (No. 6 and 7) with different initial stiffener spacings, $a/b=1.50$ and $1.00$, respectively, were built. After a first failure of girder No. 6, additional stiffeners were added to obtain ratios of $a/b=0.75$ and $0.50$ for further testing.

At loading and supporting points the stiffeners consisted of $T$-sections (ST 8 WF 25). All intermediate stiffeners were made of $4'' \times {}^{1}/_{4}''$ plates welded continuously to both sides of the web and to the compression flange. However, all stiffeners were purposely cut short one inch from the tension flange in order to study the influence of such a detail on the strength of the girder. The results of this detail investigation are published in Ref. [11]. Lateral bracing of the girders along the compression flange was provided by 10 ft. long pipes attached to the stiffeners by means of pins. The tension flange was only braced at the loading points. The bracing system is illustrated in fig. 2 showing a bending girder ready for testing.

The steel for all girders conformed to the ASTM 373–56 T Specification of the American Society of Testing Materials. It is commonly used for welded structures and corresponds closely to the ST 37.12 steel used in continental Europe. A special effort was made to procure material for the different component plates with the same yield stress. Listed in table 1 is the static yield stress of the compression flange material of girders No. 1 to 5. For the shear girders No. 6 and 7, the static yield stress of the web is given. In tests under static loading, as in the present investigation, the static yield stress is of significance. It is defined as the yield stress obtained at zero strain rate.

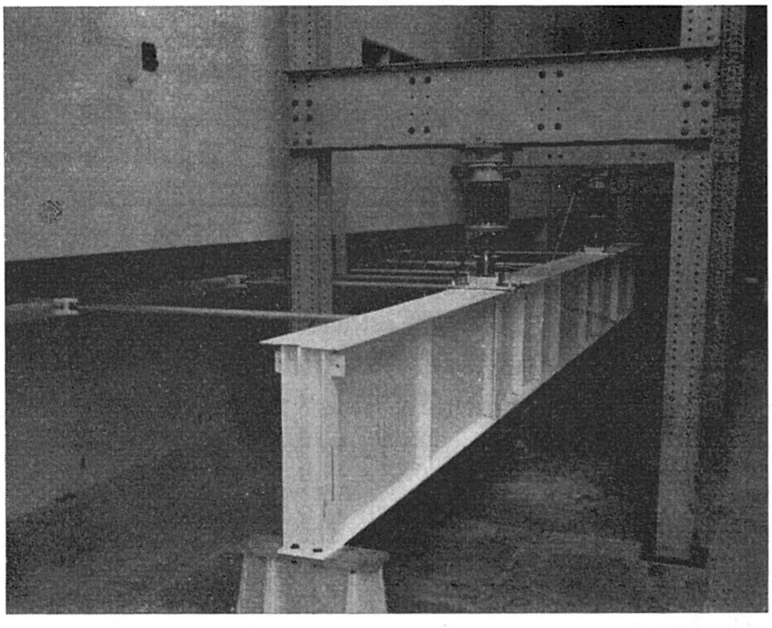

Fig. 2. Test Set-up for Bending Girders.

## 3. Testing Procedure and Results

The testing history of a girder is best illustrated by its load-deflection curve of which fig. 3 is an example. Plotted as abscissa is the midspan deflection of girder No. 4 as observed by an engineer's level. The applied jack load $P$ is the ordinate. A second ordinate indicates the computed extreme fiber stress in the top flange corresponding to the load $P$. The numbered circles in the graph mark the loading sequence at which measurements were taken. Also plotted is the theoretical elastic deflection $v_{th}$ taking into account the bending as well as the shearing deformation. The correspondence with the measured values is noteworthy.

The testing of each girder began by applying equal increments of load until the ultimate load was believed to be almost reached. For girder No. 4 this was load No. 13 at $P = 108$ kips. After unloading the girder, this load was repeated ten times (indicated by $10 \times 108$ in fig. 3) resulting in no increase of deformation. Next, the girder was loaded to its ultimate load and failure. For girder No. 4, this was caused by a sudden lateral buckling of the top flange in the long panel. This portion of the flange was then reinforced by welding a $4'' \times {}^1/_4''$ plate along both edges of the top flange over the entire length of the longer panel (fig. 4). A sufficient increase in lateral rigidity of the flange was obtained such that no further lateral deflection occurred. In a second test, which began with load No. 25 and ended with load No. 31, attention was directed to the two short panels. With a shorter stiffener spacing the lateral braces were closer together and a different type of failure could be anticipated. After pronounced yielding of the compression flange in the left-hand panel, the flange actually snapped through into the web without twisting whatsoever. Fig. 4 shows the test section after both tests were completed.

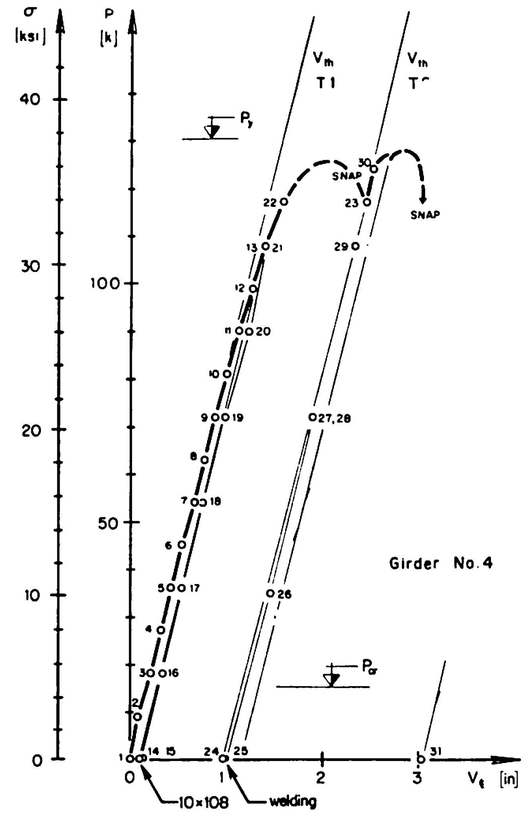


Fig. 3. Load-Deflection Curve of Girder No. 4.

In order to illustrate the behavior of the web in the course of testing, figs. 5 and 6 have been prepared. In both figures the location of the plotted observations are fixed by a coordinate system, $X$, $Y$, $Z$, as defined in the nomenclature and fig. 1.

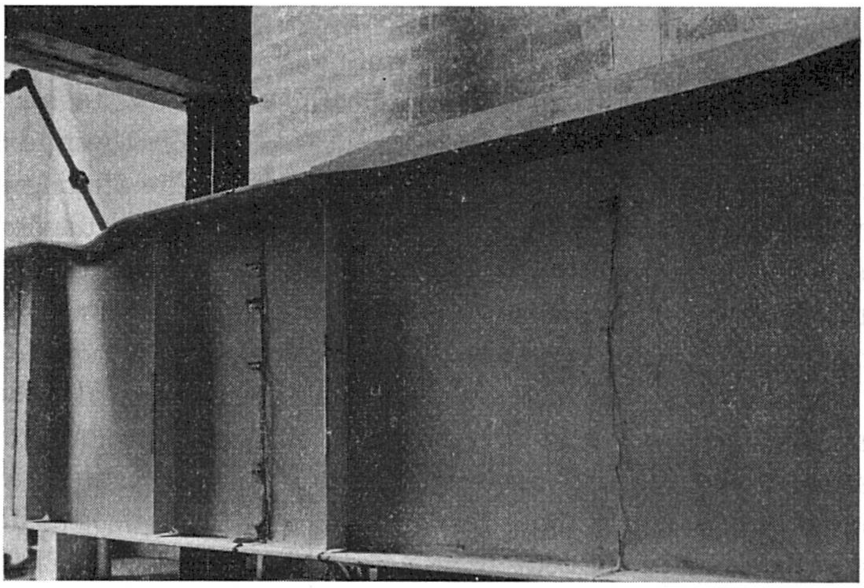

Fig. 4. Test Section of Girder No. 4 After Testing.

Lateral web deflections in the test section are shown in the upper portion of fig. 5. These deflections, $w$, are plotted in the direction of the $X$-axis at their respective locations for four different load numbers (1, 5, 9, 13; compare with fig. 3). By representing the web deflections and flange distortions to a scale 12 times that in which the test section is shown and connecting the test points with straight lines, the deflection surface of the web can easily be visualized. The graph shows that the initial distortions, load No. 1, dominated the shape of the deflection surface so strongly that the buckling mode expected according to the buckling theory could not develop. The additional web deflections up to the ultimate load are of the same order of magnitude as the initial ones, i.e. about $^1/_2$ % of the web depth.

In the lower portion of fig. 5 is shown the entire deflection history of three selected web points located below the top flange at a distance of one-fifth of the web depth. After the first unloading, a change in residual stresses usually caused deflections at zero load which were slightly different from the initial ones. However, upon reloading within the previous load range, no change in these additional permanent deflections occurred. As explained previously, the girder was loaded 10 times up to 108 kips between load No. 14 and 15. It should be pointed out that whenever the critical load, $P_{cr}$, was passed, no sudden increase of web deflection could be observed.

The web strains, as measured by electrical strain gages visible in fig. 4, are plotted in the upper portion of fig. 6. Below the stress and strain scales the outline of the girder and the strains predicted by ordinary bending theory are shown in thin lines. The dots indicate measured values and corresponding test observations are connected by the heavier lines. It becomes quite apparent that at higher loads the web portion in compression ceased to carry its full

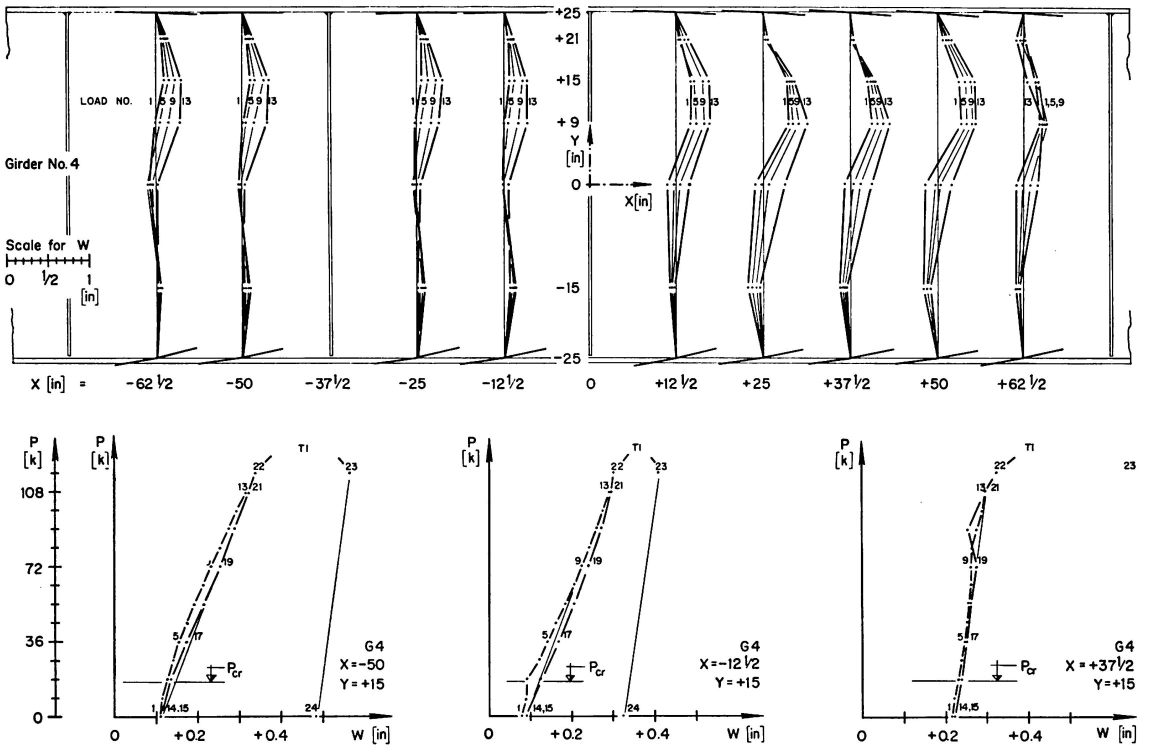


Fig. 5. Web Deflections of Girder No. 4.

share of stress according to beam theory. By deflecting laterally, as illustrated in the previous figure, the web reduced its direct or membrane stresses. At the same time, transverse plate bending stresses were created. This becomes evident by studying the load-strain chart for a particular web point as shown in the lower left-hand portion of fig. 6. The difference between a strain reading on the far side of the web surface ($Z = -{}^1/_{16}$) and the near side ($Z = +{}^1/_{16}$) is a measure of the bending stresses. Their average ($Z = 0$) is the membrane strain plotted in the uppergraph. Observing the behavior of the strain around the critical load $P_{cr}$, no sudden deviation (bifurcation) was measured although this should be expected according to the classical buckling theory.

Finally, in the last graph of figur 6, the measured strains in the extreme fibers of the top and bottom flanges are compared with the predictions of the beam theory. The actual stresses in the top flange exceeded these values by a few percent. This is not surprising because the top flange was forced to compensate for the incomplete participation of the adjacent web portion in carrying the applied moment. Since the part of the web in compression contributed relatively little to the moment of inertia of the section, the flange was able to compensate for the considerable drop in web stresses by a small increase in its own stress.

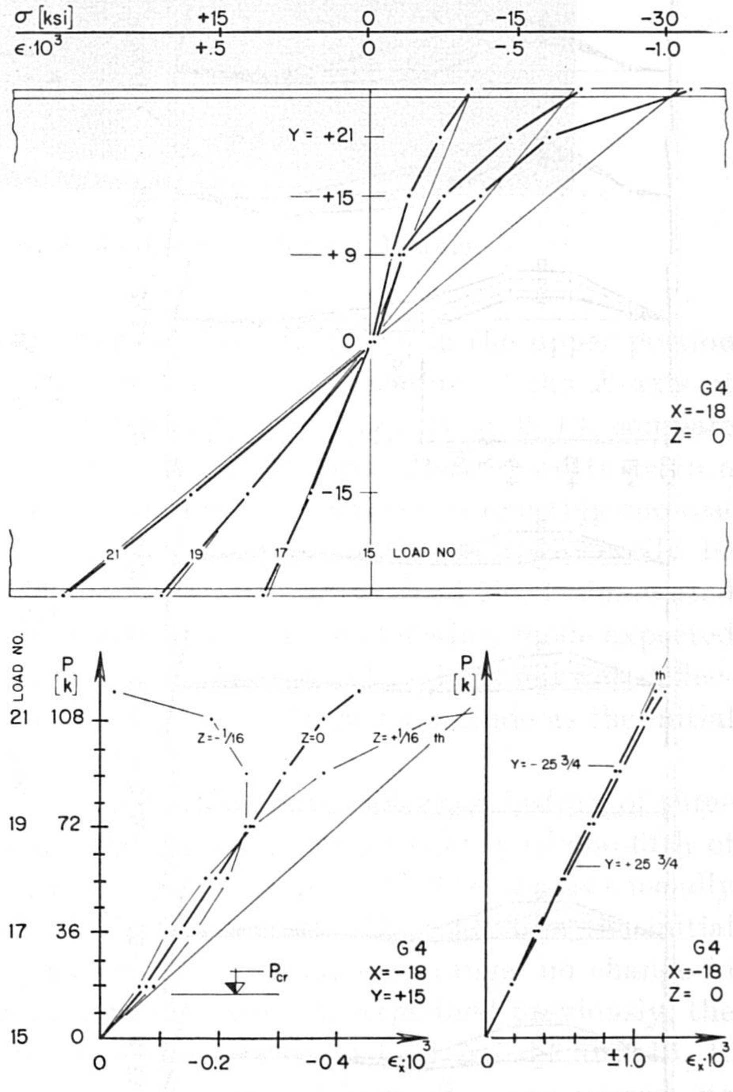


Fig. 6. Bending Strains in Girder No. 4.

Table 2 summarizes the fifteen ultimate loads obtained in testing the seven girders. The failures of the bending girders No. 2 to 5 in a first test, $T\,1$, were due to lateral buckling of the compression flange within the long panel as just described for girder No. 4. Upon reinforcing, as indicated pictorially in the third column of table 2, failure in test $T\,2$ was forced into a short panel by buckling locally, i. e., local crippling of the pipe flange for girders No. 3 and 5, and twisting of the flange for girder No. 2. The two failures produced on each girder did not overlap and thus the two tests furnished truly independent results.

Girder No. 1 had a wide top flange with a width to thickness ratio $2c/d = 48$. In the first test $T\,1$ the top flange deformed into a wave pattern in accordance with the classical buckling theory. After reducing the flange width by flame

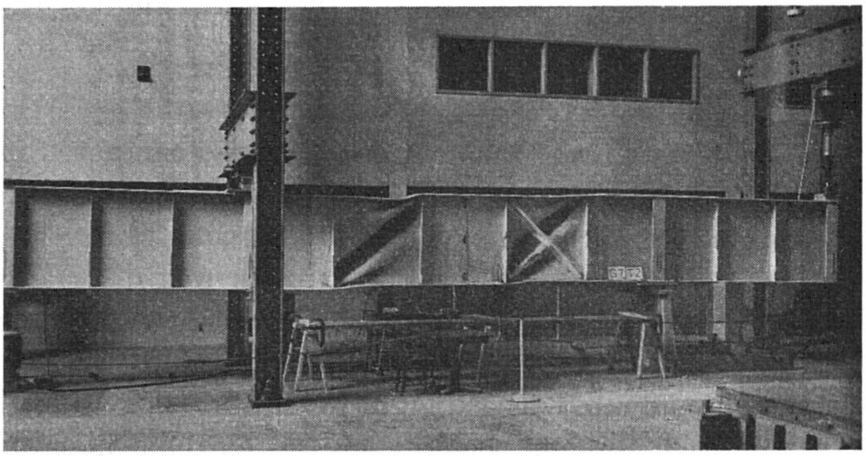

Fig. 7. Shear Girder No. 7 After Testing.

*Table 2. Summary of Critical Loads $P_{cr}$, Yield Loads $P_y$, and Ultimate Loads $P_u$.*

| Girder | Test No. | Condition | Theoretical $P_{cr}$ (kips) | Theoretical $P_y$ (kips) | Exper. $P_u$ (kips) |
|---|---|---|---|---|---|
| 1 | T 1 | 2c = 20.6″ | 70.1 | 130.9 | 81 |
| | T 2 | 2c = 13.6″ | 41.9 | 100.8 | 72 |
| 2 | T 1 | | 74.1 | 148.8 | 135 |
| | T 2 | | | | 144 |
| 3 | T 1 | | 82.1 | 115.6 | 130 |
| | T 2 | | | | 136 |
| 4 | T 1 | | 15.3 | 130.1 | 118 |
| | T 2 | | | | 125 |
| 5 | T 1 | | 17.0 | 104.9 | 110 |
| | T 2 | | | | 124 |
| 6 | T 1 | | 27.4 | 193.3 | 116 |
| | T 2 | | 51.9 | | 150 |
| | T 3 | | 97.6 | | 177 |
| 7 | T 1 | | 37.6 | 196.0 | 140 |
| | T 2 | | | | 145 |

= reinforced panel

cutting to $2c/d = 32$, the girder was reloaded in a second test $T\,2$. Failure occurred again by excessive twisting of the top flange.

In the shear tests of girders No. 6 and 7 yield bands developed along tension diagonals. Fig. 7 shows a photograph of girder No. 7 after the second test. The right hand panel was reinforced by a compression diagonal after failing in a first test. Three ultimate loads for three different stiffener spacings were obtained from girder No. 6 as indicated in table 2.

The last three columns of table 2 list two theoretical and one experimental load $P$. The line of action of $P$ is shown in fig. 1a and 1b. The three loads are defined as follows:

$P_{cr}$, the critical load, is the web buckling load. It was computed in the usual manner (Ref. [7], [9]) by taking a buckling coefficient $k = 23.9$ for bending or $k = 5.34 + 4/\alpha^2$ for shear provided $\alpha \geqq 1$. In computing the $P_{cr}$ of the shear girders the influence of bending stresses was disregarded. In the cases where the neutral axis did not coincide with the middle of the web depth the computation proceeded according to Ref. [8].

$P_y$, is the yield load computed according to the beam theory. For the bending girders it initiated nominal yielding at the extreme fiber of the compression flange. At midspan of the shear girders, yielding was first reached at the neutral axis. For these two girders $P_y$ was computed with the maximum shear stress equal to $\sigma_y/\sqrt{3}$, where $\sigma_y$ was the yield stress of the web material.

$P_u$, the ultimate load, is the highest observed jack load which could be maintained on a girder and hence was observed at zero straining speed. The maximum registered load in the process of testing was sometimes slightly higher depending on the rate of straining.

## 4. Ultimate Versus Critical Loads

In order to visualize the strength of the girders beyond the computed critical load, figs. 8 and 9 were prepared. Ultimate loads anywhere between 15% and 800% above the conventionally computed critical loads were obtained. This should be evidence enough that the load carrying capacity of an ordinary transversely stiffened plate girder can not be based on the web buckling load. There is no consistent ratio between the ultimate load and the web buckling load.

Certainly, the conditions of the tested web panels differed in two ways from the assumptions on which the buckling computations were based. First, the web was not truly plane initially. As explained in the discussion of figs. 5 and 6, this fact made it impossible to determine experimentally the web buckling load. Second, the actual boundary conditions differed from the assumed simply supported ones. Considering for a moment the bending girders,

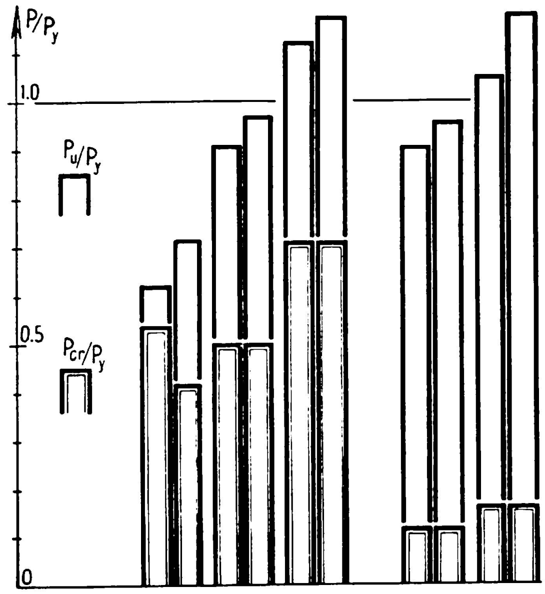


| Girder | G1 | | G2 | | G3 | | | G4 | | G5 | |
|---|---|---|---|---|---|---|---|---|---|---|---|
| Test | T1 | T2 | T1 | T2 | T1 | T2 | | T1 | T2 | T1 | T2 |
| a/b | 0.75 1.50 | | 1.5 | .75 | 1.5 | .75 | | 1.5 | .75 | 1.5 | .75 |
| b/t | 185 | | | | | | | 388 | | | |

Fig. 8. Comparison of Ultimate and Critical Loads of Bending Tests.

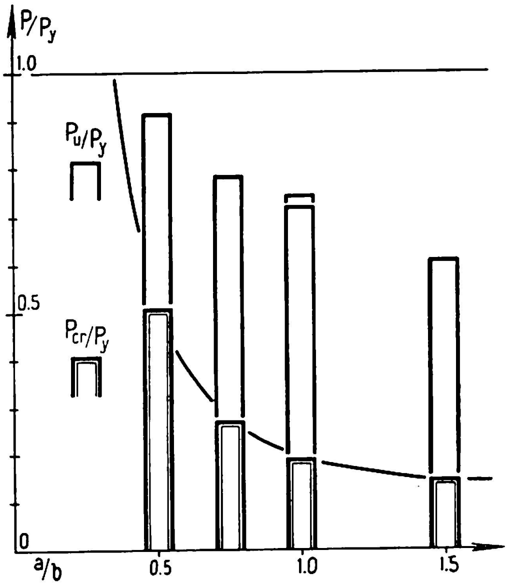


| Girder | G 6 | G 6 | G 7 | | G 6 |
|---|---|---|---|---|---|
| Test | T 3 | T 2 | T1-T2 | | T 1 |
| b/t | 259 | 259 | 255 | | 259 |

Fig. 9. Comparison of Ultimate and Critical Loads of Shear Girders.

all three panels within the test section became critical at nearly the same load such that a panel could get little restraint at its loaded edges. However along the flanges the boundary conditions for girders No. 2 to 5 were more favorable, approaching full restraint. It can be shown, however, that for an aspect ratio $\alpha \geqq 0.5$ the error in choosing pinned instead of totally fixed boundaries along the unloaded edges leads to an increase of less than 100% in the critical buckling load. Incidentally, this holds for all loading cases, such as bending, shear, compression, or their combinations. The above mentioned percentage includes possible beneficial effects of stiffener spacings which do not coincide with the half wave length of the unstiffened plate. Making use of all these refinements in the computation of $P_{cr}$ would not correct the inconsistency between the observed ultimate loads and the critical loads.

## 5. Discussion

### *a) Girders in Pure Bending*

In reviewing fig. 6, showing the web strains of a bending girder, attention was directed to the post-buckling strength of the web plate. This phenomenon is generally advanced as an explanation for the strength beyond the critical load. It should be noted, however, that even if the web plate had no post-buckling strength at all the load could still be increased beyond $P_{cr}$. In this case the web forces would be transferred to the flange thus compensating for the moment resistance lost in the web.

Considering these facts, the ultimate loads obtained from the bending girders shall be studied now. The first group, composed of girders No. 1, 2 and 3, varied only in the shape of the compression flange. All three girders had the same web thickness, web depth, stiffener spacing and loading condition. Nevertheless, their ultimate loads differed greatly. Girder No. 1 was designed such that the critical stress $\sigma_{cr}$ in the top flange was just slightly above $\sigma_{cr}$ for the web. Since the flange plate had free edges, it could not transfer forces to other elements. Hence, it collapsed soon after $P_{cr}$ was reached which led to failure of the entire girder. The top flange of girder No. 2 was built with the same cross sectional area as all other bending girders but proportioned such that plate buckling could not occur before strain hardening. Ultimate load was reached when the flange started to buckle laterally. Girder No. 3 had a tubular top flange with equal bending rigidities in all directions and excellent local buckling characteristics. Its use resulted in ultimate loads beyond the yield load. In the second group of tests, girders No. 4 and 5 duplicated girders No. 2 and 3 respectively, except for the web slenderness which was doubled. This increase led to computed critical loads which were only one quarter of the corresponding values for girders No. 2 and 3. Nevertheless, the corresponding ultimate loads, as seen in fig. 8, were practically the same. Hence, it must be concluded that, at least in this range, the web slenderness ratio does not affect the strength.

### *b) Girders in High Shear*

In the shear girder tests the ultimate loads also exceeded the critical loads considerably (fig. 9). As in the case of bending the web was able to rearrange its forces. At high shear, tension diagonals developed and the girders acted similar to a truss (fig. 7). However, this action is entirely different from the assumptions on which the buckling theory is based. Therefore, the theory is also unable to predict the carrying capacity of girders subjected to shear.

### *c) General Considerations*

It has been pointed out repeatedly that a web panel should not be considered as an isolated element. It is framed by the flanges and transverse stiffeners, referred to as the supporting frame. The presence of this frame allows the web to change the stress pattern predicted by the beam theory to a more favorable one. Besides the web's own post-buckling strength, this transfer is the important and governing contribution to the post-buckling strength of conventionally designed plate girders. It is therefore of utmost importance to investigate the strength of this supporting frame. A study, now being undertaken, shall include these considerations in the analysis of the static strength of plate girders.

## 6. Acknowledgements

This investigation has been carried out in the course of research on "Welded Plate Girders" at Fritz Engineering Laboratory, Lehigh University, Bethlehem, Pennsylvania, U.S.A. Professor W. J. Eney is director of the Laboratory.

The project is sponsored jointly by the American Institute of Steel Construction, the Pennsylvania Department of Highways, the U.S. Bureau of Public Roads and the Welding Research Council. It is supervised by a committee under the chairmanship of Mr. E. L. Erickson, Chief, Bridge Division, U.S. Bureau of Public Roads. The help of Messrs. B.T. Yen and J. A. Mueller in conducting the tests is gratefully acknowledged.

## 7. References

1. G. Wästlund and St. Bergmann, "Buckling of Webs in Deep Steel I-Girders". Report of the Institution of Structural Engineering and Bridge Building, Stockholm.
2. Ch. Massonnet, «Recherches expérimentales sur le voilement de l'âme des poutres à âme pleine». Bulletin du Centre d'Etudes, Tome 5, 1951; pp. 67—240, ou A.I.P.C., Publ. prél., 4e Congrès Cambridge-Londres, 1952; pp. 539—555.
3. Ch. Massonnet, «Essais de voilement sur poutres à âme raidie». A.I.P.C., Mém., Vol. 14, Zurich, 1954; pp. 125—186, ou Acier, No. 2, février 1955; pp. 3—12.
4. E. Longbottom and J. Heyman, "Experimental Verification of the Strengths of Plate Girders Designed in Accordance with the Revised British Standard 153: Tests on Full Size and on Model Plate Girders". The Institution of Civil Engineers, Great George Street, Westminster, London S.W. 1, Struct. Paper No. 49, 1956; pp. 463 to 486.
5. K. C. Rockey and F. Jenkins, "The Behavior of Web Plates of Plate Girders Subjected to Pure Bending". Structural Engineer, Vol. 35, No. 5, 1957; pp. 176—189.
6. G. Winter, "Post-Buckling Strength of Plates in Steel Design." I.A.B.S.E., F. Rep., 1952; p. 268.
7. F. Bleich, "Buckling Strength of Metal Structures" (Book). McGraw-Hill Company, New York, London, and Toronto, 1952.
8. F. Stüssi, C. F. Kollbrunner und W. Wanzenried, «Ausbeulen rechteckiger Platten unter Druck, Biegung und Druck mit Biegung». Inst. f. Baust. a. d. ETH, Mitt. Nr. 26, Verlag Leemann, Zürich, 1953.
   «Tabellen der Beulwerte *k*.» Schweizer Stahlbau Verband, Zürich, Mai 1953.
9. Deutscher Normenausschuß «DIN 4114, Blatt 1 und 2». Beuth-Vertrieb GmbH, Berlin W 15 und Köln, 1952 und 1953.
10. B. Thürlimann, "Strength of Plate Girders". A.I.S.C. National Engineering Conference, Proceedings 1958, American Institute of Steel Construction, 101 Park Avenue, New York 17, New York.
11. K. Basler and B. Thürlimann, "Plate Girder Research". A.I.S.C. National Engineering Conference, Proceedings 1959, American Institute of Steel Construction, 101 Park Avenue, New York 17, New York.

## 8. Nomenclature

$a$ Distance between transverse stiffeners.
$b$ Depth of girder web.
$c$ Half the flange width.
$d$ Thickness of flange.
$t$ Thickness of web.
$v$ Girder deflection.
$w$ Lateral web deflection.
$P$ Load, defined in fig. 1a and chapter 3.
$T$ Test (e.g. $T$ 2 is "second test").

$X, Y, Z$ Coordinates (in inches), as shown in fig. 1.
$\alpha = a/b$ Panel length to panel depth (aspect ratio).
$\beta = b/t$ Web depth to web thickness (slenderness ratio).
$\epsilon$ Strain.
$\sigma$ Normal stress, positive if tension.
$\tau$ Shear stress.
$\zeta = \tau/\sigma$ Ratio of maximum values of shear to normal stress at center line of girders.

*Subscripts*

$cr$ = critical, $y$ = yield, $u$ = ultimate, $th$ = theoretical.

*Conversion factors*

Force: 1 kip [k] = 1000 pounds [lbs] = 454 kilograms [kg].
Length: 1 foot [ft] or ['] = 12 inches [in] or ["] = 30,5 centimeters [cm].
Stress: 1 kip per square inch [ksi] = 0.703 kilograms per square millimeter [kg/mm$^2$].


### Summary

Fifteen ultimate load tests carried out on seven fullsize plate girders show that the classical buckling theory for webs is unable to predict the carrying capacity of such members. The reason for this lies in the fact that a web panel in a plate girder is surrounded by flanges and stiffeners which participate in the functions of the web.

### Résumé

Quinze essais de charge sur sept grandes poutres à âme pleine montrent que la théorie classique du voilement pour les âmes n'est pas en mesure de déterminer la résistance limite de ces éléments.

La raison réside dans le fait que l'âme est entourée d'ailes et de raidisseurs verticaux prenant part aux fonctions de l'âme.

### Zusammenfassung

Fünfzehn Tragversuche, ausgeführt an sieben großen Vollwandträgern, zeigen, daß die klassische Beultheorie für Trägerstege nicht in der Lage ist, die Tragfähigkeit solcher Konstruktionsteile zu bestimmen. Der Grund liegt in der Tatsache, daß ein Stegblech eingerahmt ist von Flanschen und Quersteifen, welche an den Funktionen des Steges teilnehmen.